Supplementary Information

# Building mechanism of a high open-circuit voltage in all-solution-processed tandem polymer solar cell

Jaemin Kong, Jongjin Lee*, Geunjin Kim, Hongkyu Kang , Youna Choi and Kwanghee Lee*

*School of Materials Science & Engineering, Research Institute for Solar and Sustainable Energies (RISE), Gwangju Institute of Science and Technology, Gwangju 500-712, South Korea*

*E-mail: bandy1@gist.ac.kr, Klee@gist.ac.kr*

## 1. J-V characteristics of a back half-cell incorporated with $TiO_x$/PEDOT:PSS interlayers

When the interlayers were incorporated in P3HT back half-cell, the half-cell exhibited normal value of $V_{OC}$ (~ 0.6V), but it had a low fill factor due to high series resistance. The reason why $V_{OC}$ of the back half-cell from the beginning had a normal value of 0.6V was the P3HT photoactive layer was put in the asymmetric contact potential derived from a work function difference between PEDOT:PSS (~ 0.50eV) and Al (~ 0.43eV). However, the extracted charges seemed to meet electrical barriers exhibited as high series resistance, as shown in Fig. S1. This might arise from the $TiO_x$/PEDOT:PSS interlayer, because the high series resistance was significantly decreased from 0.33 $k\Omega \cdot cm^2$ to 15.0 $\Omega \cdot cm^2$ after post-treatments (see table S1). This result was analogous to the case of SDT-BT front half-cell, which was incorporated with $TiO_x$/PEDOT:PSS interlayers, with respect to the formation of better recombination junction.

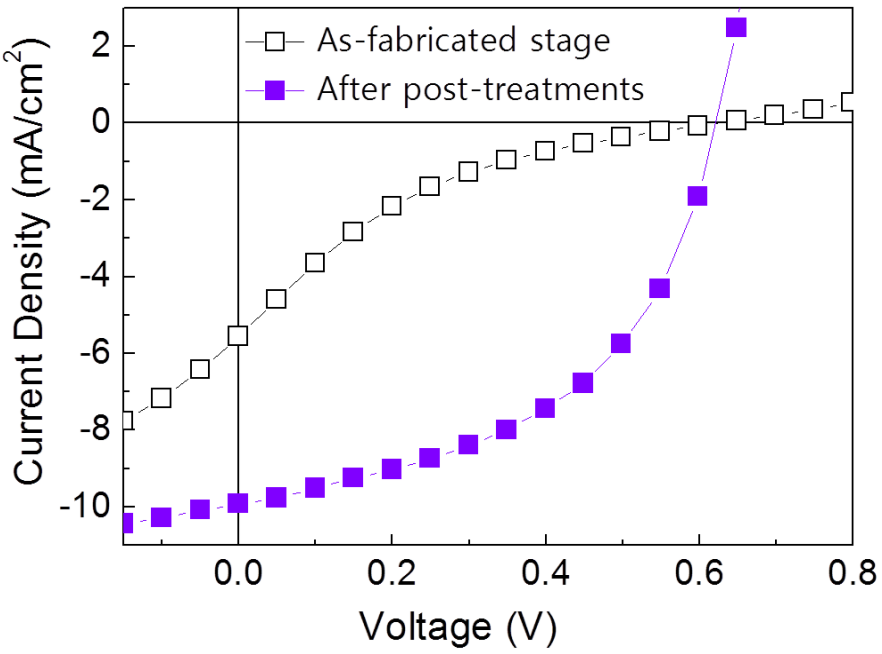


**Fig. S1** J-V characteristics of a back half-cell incorporated with $TiO_x$/PEDOT:PSS interlayers before and after post-treatments.

| | $V_{oc}$ (V) | $J_{sc}$ (mA cm$^{-2}$) | *FF* | *PCE* (%) | $R_s$ (Ω·cm$^2$) | $R_{sh}$ (Ω·cm$^2$) |
|---|---|---|---|---|---|---|
| *As-fabricated* | 0.63 | 5.56 | 0.12 | 0.43 | 330 | 67.0 |
| *Post-annealing & illumination* | 0.62 | 9.93 | 0.50 | 3.05 | 15.0 | 278 |

**Table S1** Cell parameters of a back half-cell incorporated with $TiO_x$/PEDOT:PSS interlayers before and after post-treatments.

**2. J-V characteristics of a front cell, back cell, and hole-only device**

When the injection current characteristics of each subcell were compared with those of a hole-only device (ITO/PEDOT:PSS/P3HT:$PC_{71}BM$/PEDOT:PSS/Au), the front half-cell behaved as a hole-only device in pristine condition (see **Fig. S2**). However, the J-V characteristics of the front half-cell gradually approached those of an appropriately working back half-cell as the post-treatment processes were implemented.

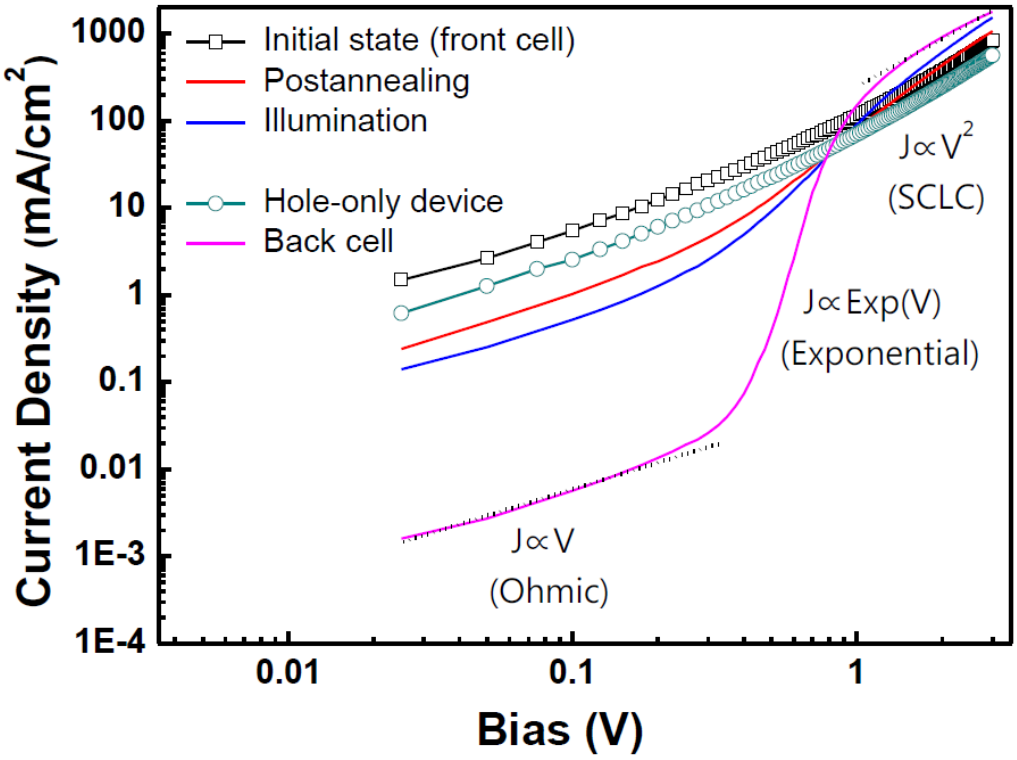


**Fig. S2** The log-log plots of the current density versus bias for the front half-cell in various stages, including J-V curves for the hole-only device and the back half-cell.

### 3. Comparison study for the post-thermal annealing process

Thermal annealing without Al top electrode did not affect the $V_{OC}$ recovery, as shown in **Fig. S3 (a)**. To identify the role of the Al in the post-annealing process, devices with Al and Au electrodes in a tandem structure were compared. By changing the metal used for the top cathode, one can change the electric field induced by the difference in the work function between the top and bottom electrodes across several layers. In **Fig. S3 (b)**, a distinctive difference in the $V_{OC}$ recovery can be observed between the two different top electrodes, even with the same post-annealing condition. The $V_{OC}$ of the as-prepared tandem cell with the Al electrode is clearly increased by post-annealing. In contrast, the $V_{OC}$ of the device with the Au electrode is nearly unchanged after post-annealing. Because the work function of Au is nearly the same as that of the bottom PEDOT:PSS/ITO electrode, there is no appreciable electric field between the Au cathode and the PEDOT:PSS/ITO anode. This electric field dependence on the $V_{OC}$ recovery was independently confirmed by the BTS experiment (see text), as shown in **Fig. 5 (a)**. Although an Al top electrode was employed, the $V_{OC}$ depends on the polarities of an external bias. Thus, we could conclude that the effect from the Al cathode is in reality due to the electric field.

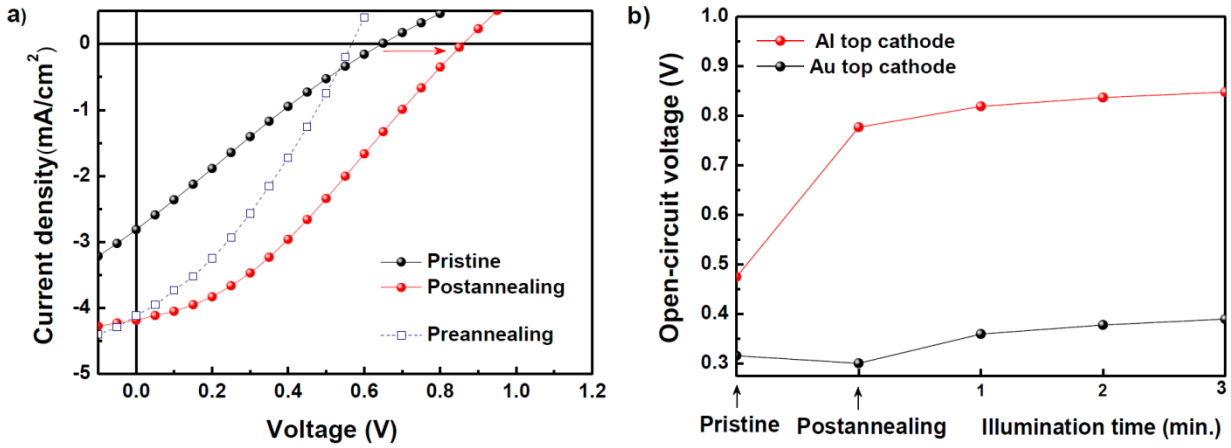


**Fig. S3** (a) The current density versus voltage plots of a pre-annealed device (without an Al electrode) compared with a post-annealed device (with an Al electrode). (b) The $V_{OC}$ changes of the devices during post-treatments with respect to the top cathode materials and illumination.

**4. Permittivity ($\varepsilon_s$) of $TiO_x$ before and after UV-illumination**

Capacitance-Voltage (C-V) measurement was performed to obtain the permittivity ($\varepsilon_s$) of $TiO_x$ in a simple MIM device structure (ITO/$TiO_x$/Al) by Agilent 4155B Semiconductor Parameter Analyzer. Thickness of the $TiO_x$ film is ca. 22nm measured by surfcorder ET3000, and the active area of the device is 4.64$mm^2$ defined by the area of top metal electrode. The frequency was set to 10 kHz, and the external bias was swept from reverse to forward. The permittivity of $TiO_x$ was calculated by simple equation, $C= \varepsilon_s/W$, where C is a capacitance, $\varepsilon_s$ is a permittivity of the medium ($TiO_x$), and W is a plate separation of conventional capacitor. The C is taken as an average value within the voltage sweep region (-5V to +5V). Before and after UV-illumination the permittivity of $TiO_x$ was slightly changed from 80.52x$10^{-12}$ F/m to 71.06x$10^{-12}$ F/m.

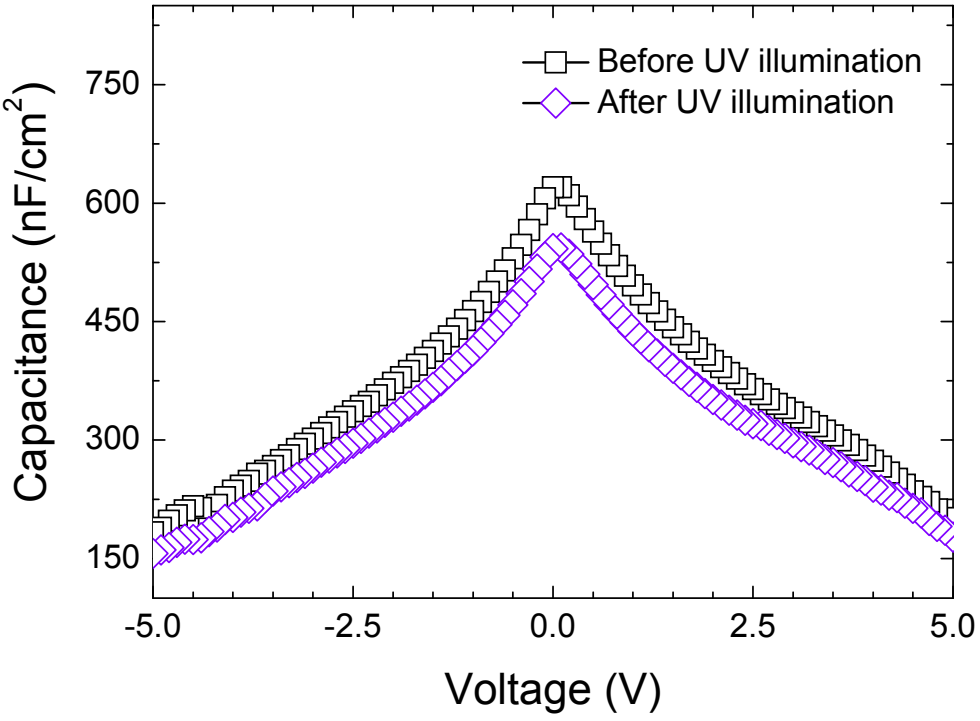


**Fig. S4** C-V data for the $TiO_x$ layer in a simple MIM configuration.